

Regularizing Subspace Redundancy of Low-Rank Adaptation

Yue Zhu*
 Dalian University of
 Technology
 Dalian, China
 zhuyuedlut@gmail.com

Jiawen Zhu
 Dalian University of
 Technology
 Dalian, China
 jiawen@mail.dlut.edu.cn

Lu Zhang
 Dalian University of
 Technology
 Dalian, China
 zhanglulu@dlut.edu.cn

Haiwen Diao*
 Dalian University of
 Technology
 Dalian, China
 diaohw@mail.dlut.edu.cn

Yunzhi Zhuge
 Dalian University of
 Technology
 Dalian, China
 zgyz@dlut.edu.cn

Ying Zhang
 WeChat Vision, Tencent Inc.
 Dalian, China
 yinggzhang@tencent.com

Shang Gao*
 Dalian University of
 Technology
 Dalian, China
 gs940601k@mail.dlut.edu.cn

Shuai Hao
 Dalian University of
 Technology
 Dalian, China
 shuiahao@mail.dlut.edu.cn

Jiazu Yu
 Dalian University of
 Technology
 Dalian, China
 yujiazu@mail.dlut.edu.cn

Xu Jia
 Dalian University of
 Technology
 Dalian, China
 xjia@dlut.edu.cn

Huchuan Lu†
 Dalian University of
 Technology
 Dalian, China
 lhchuan@mail.dlut.edu.cn

Abstract

Low-Rank Adaptation (LoRA) and its variants have delivered strong capability in Parameter-Efficient Transfer Learning (PETL) by minimizing trainable parameters and benefiting from reparameterization. However, their projection matrices remain unrestricted during training, causing high representation redundancy and diminishing the effectiveness of feature adaptation in the resulting subspaces. While existing methods mitigate this by manually adjusting the rank or implicitly applying channel-wise masks, they lack flexibility and generalize poorly across various datasets and architectures. Hence, we propose **ReSoRA**, a method that explicitly models redundancy between mapping subspaces and adaptively **Regularizes Subspace** redundancy of **Low-Rank Adaptation**. Specifically, it theoretically decomposes the low-rank submatrices into multiple equivalent subspaces and systematically applies de-redundancy constraints to the feature distributions across different projections. Extensive experiments validate that our proposed method consistently facilitates existing state-of-the-art PETL methods across various backbones and datasets in vision-language retrieval and standard visual classification benchmarks. Besides, as a training supervision, **ReSoRA** can be seamlessly integrated into existing approaches in a plug-and-play manner, with no additional inference costs. Code is publicly available at: <https://github.com/Lucenova/ReSoRA>.

*Equal Contribution

†Corresponding Authors

Permission to make digital or hard copies of all or part of this work for personal or classroom use is granted without fee provided that copies are not made or distributed for profit or commercial advantage and that copies bear this notice and the full citation on the first page. Copyrights for components of this work owned by others than the author(s) must be honored. Abstracting with credit is permitted. To copy otherwise, or republish, to post on servers or to redistribute to lists, requires prior specific permission and/or a fee. Request permissions from permissions@acm.org.

MM '25, Dublin, Ireland

© 2025 Copyright held by the owner/author(s). Publication rights licensed to ACM. ACM ISBN 979-8-4007-2035-2/2025/10
<https://doi.org/10.1145/3746027.3755359>

CCS Concepts

- Computing methodologies → Transfer learning.

Keywords

Parameter-efficient transfer learning; low-rank adaption; subspace regularization; plug-and-play

ACM Reference Format:

Yue Zhu, Haiwen Diao, Shang Gao, Jiazu Yu, Jiawen Zhu, Yunzhi Zhuge, Shuai Hao, Xu Jia, Lu Zhang, Ying Zhang, and Huchuan Lu. 2025. Regularizing Subspace Redundancy of Low-Rank Adaptation. In *Proceedings of the 33rd ACM International Conference on Multimedia (MM '25), October 27–31, 2025, Dublin, Ireland*. ACM, New York, NY, USA, 10 pages. <https://doi.org/10.1145/3746027.3755359>

1 Introduction

Recently, large fundamental models [3, 11, 12, 20, 52] have exhibited remarkable generalization capabilities across natural language processing (NLP), computer vision (CV), and vision-language (VL) tasks. Nevertheless, fine-tuning all network parameters is computationally and storage-intensive, and with limited data scales, it may impede adaptation and result in suboptimal performance.

To address this, Parameter-Efficient Transfer Learning (PETL) techniques [5, 29, 30] have been increasingly gaining attention across a range of downstream applications [13, 63]. They typically freeze most model parameters, either inserting small trainable blocks [7, 28, 56] into the pre-trained model or selectively adjusting a limited subset of parameters [25, 35, 64]. They significantly reduce trainable parameters while preserving or improving model capability. Among them, Low-Rank Adaptation (LoRA) [22, 29, 31, 67] stands out for its simplicity and efficiency. It assumes that weight updates during the fine-tuning process have a low intrinsic rank and adapts by optimizing the corresponding decomposition matrices. During inference, the low-rank matrices can be integrated seamlessly into the pre-trained backbone weights through reparameterization, incurring no additional prediction latency.

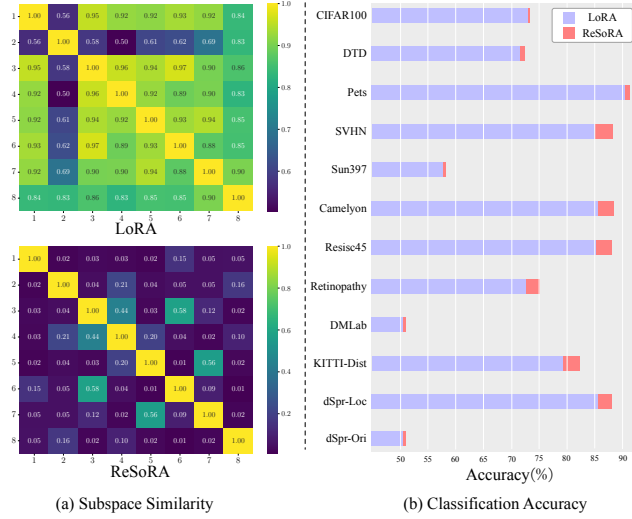


Figure 1: Comparison between our ReSoRA and LoRA [29]: (a) subspace redundancy regularization over decoupled query matrix in the last ViT layer on SVHN; (b) prediction accuracy improvements across various classification benchmarks.

Although effective, LoRA shows significant redundancy in its low-rank adaptation matrices. To quantify it, we decompose the mapping function into multiple subspace components, where high inter-subspace redundancy means more overlap and less diversity. Figure 1 shows strong correlations between LoRA’s subspaces, indicating poor disentanglement. Combined with limited gains, this highlights the need for improved training strategies that suppress similarity and encourage orthogonality across projection spaces.

Recent studies [16, 67, 68] aim to build more compact and efficient mapping spaces. AdaLoRA [67] applies SVD to reformulate adaptation matrices and prunes singular values by importance, while SoRA [16] uses a gated mechanism with proximal gradient descent and ℓ_1 regularization to remove inactive components. Although these approaches reduce redundancy and improve efficiency, they remain constrained by fixed ranks and show limited flexibility and generalization across datasets and architectures.

In this paper, we present ReSoRA that decomposes the adaptive output space into multiple subspaces and introduces a tailored subspace regularization term. We systematically identify the most effective regularization strategies to enforce mapping constraints and reduce redundancy across subspaces, improving representational capacity and enabling better domain adaptation.

Our contributions can be summarized as follows:

- We explicitly decompose the low-rank mapping space into multiple subspaces and effectively regularize redundancy to promote orthogonality among them, offering a new perspective on facilitating low-rank adaptation.
- We introduce ReSoRA, a simple yet effective method that serves as a plug-and-play anti-redundancy regularizer during training. It consistently enhances various state-of-the-art PETL works, e.g., LoRA [29], FacT [31], MoSLoRA [59], and DTL [22], without any inference overhead.

- We perform extensive experiments on various backbones and datasets in visual language retrieval and standard visual classification benchmarks, demonstrating the effectiveness and robustness of the proposed ReSoRA.

2 Related Work

2.1 Parameter-Efficient Transfer Learning

Parameter-Efficient Transfer Learning (PETL) [39, 70] has been developed to selectively fine-tune a small subset of parameters, achieving high efficiency. Among them, partial tuning approaches [35, 64] adapt pre-trained models by training only a subset of parameters. BitFit [64] updates only bias terms, while LayerNorm Tuning [35] adjusts parameters within Layer Normalization layers. Besides, prompt-tuning methods [30, 33] integrate trainable prompt tokens into the input sequence, enabling task-specific learning without modifying pretrained weights. Furthermore, adapter-based methods [15, 23] insert lightweight modules within transformers for adaptation. Notably, Adapter Re-composing [18], RLRR [19], and Householder Adaptation [17] achieve strong performance by improving parameter efficiency via multiple adapter compositions, residual low-rank tuning, and Householder transformations.

A notable PETL method is LoRA [29], which models the weight update matrix ΔW in a linear layer as a low-rank approximation. Building on this, subsequent studies have proposed advanced techniques to further improve adaptation, including factorized bilinear matrices [31], compactor decomposition [45], and tensor factorization [6]. Other works [22] decouple weight updates from the backbone via a lightweight side network. Our ReSoRA naturally complements this paradigm, integrating seamlessly with various LoRA-like methods while adding no inference overhead.

2.2 Regularization in Low-Rank Adaptation

Low-rank adaptation reduces the number of trainable parameters by restricting weight updates to rank- r subspaces. While commonly used ranks ($r = 8, 16, 32$) are typically chosen based on empirical heuristics, the optimal rank can vary with task complexity and requirements. Selecting an appropriate r is crucial—an excessively high rank may introduce redundancy within low-rank matrices, leading to potential inefficiency and performance degradation.

To address it, one group of methods focuses on selecting an appropriate rank to balance expressiveness and efficiency. For instance, In-creLoRA [66] incrementally increases the rank based on parameter importance scores. AdaLoRA [67] adopts Singular Value Decomposition (SVD) to parameterize rank adaptation, while AutoLoRA [68] leverages meta-learning to adjust ranks automatically during training. Besides, another group aims to enhance the independence and diversity of low-rank matrices. Among them, MLAE [58] introduces a cellular decomposition strategy that factorizes a low-rank matrix into independent rank-1 components. SiRA [71] employs a Sparse Mixture of Experts (SMoE) to boost LoRA’s capacity, and MoSLoRA [59] uses a learnable mixer to more flexibly combine diverse subspaces. Orthogonally, ReSoRA decomposes low-rank submatrices into equivalent subspaces and enforces de-redundancy constraints across their feature distributions, which can seamlessly cooperate with various LoRA-like methods during fine-tuning.

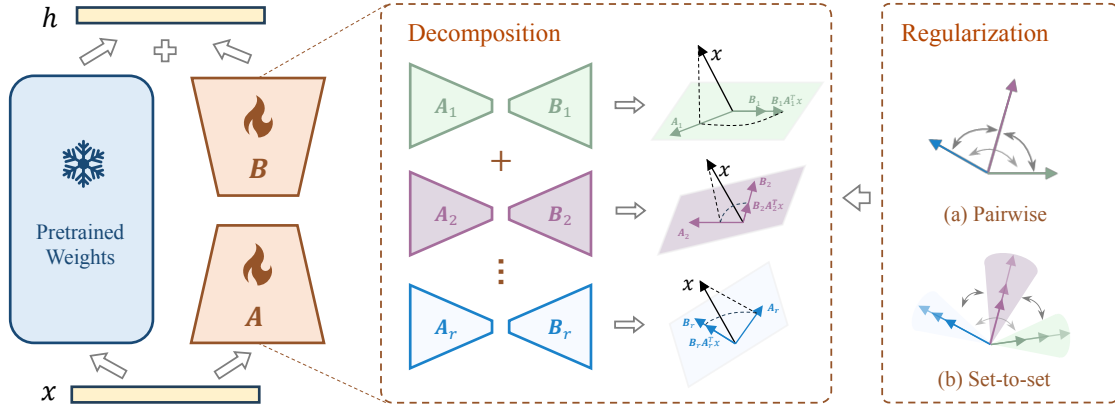


Figure 2: Overview of our proposed ReSoRA. The original output space is decomposed into a combination of multiple subspaces. To reduce subspace redundancy, we adopt a carefully designed regularization that includes pairwise and set-to-set terms.

3 Methodology

In this paper, we present ReSoRA, a general and adaptive framework designed to enhance low-rank adaptation. At its core is subspace redundancy regularization, a family of techniques that explicitly mitigates redundancy and promotes representation diversity across decomposed subspaces. Our ReSoRA is flexible and extensible, supporting both pairwise or set-to-set regularization items.

3.1 Subspace Projection Decomposition

To demonstrate the effectiveness of our ReSoRA, we focus on enhancing the widely-used LoRA [29, 59] method by incorporating ReSoRA as regularization. Concretely, LoRA assumes that weight updates during fine-tuning occur in a low-dimensional subspace and approximates these updates as the product of two low-rank matrices. Formally, given a pre-trained weight matrix $W_0 \in \mathbb{R}^{d_{in} \times d_{out}}$, where d_{in} and d_{out} denote the input and output dimensions respectively, the fine-tuned weight W can be expressed as:

$$W = W_0 + \Delta W = W_0 + BA, \quad (1)$$

where BA is a low-rank decomposition of the adaptive weight increment ΔW . Hence $B \in \mathbb{R}^{d_{in} \times r}$ and $A \in \mathbb{R}^{r \times d_{out}}$, with $r \ll \min\{d_{in}, d_{out}\}$. During the training phase, the pre-trained weight W_0 remains unchanged, while the parameters in A and B are trainable. Subsequently, ΔW can be merged into W_0 without introducing any latency during inference. To investigate the redundancy in low-rank adaptation, we first perform decomposition on the parameter ΔW . Specifically, both A and B can be decomposed into rank-1 subspaces r : $A = [A_1, A_2, \dots, A_r]^T$, $B = [B_1, B_2, \dots, B_r]$, where $A_i \in \mathbb{R}^{d_{in} \times 1}$ and $B_i \in \mathbb{R}^{d_{out} \times 1}$ for $1 \leq i \leq r$. Thus, the adaptive weight in Eq. (1) can be explicitly decomposed as:

$$\begin{aligned} W &= W_0 + W_1 + W_2 + \dots + W_r \\ &= W_0 + B_1 A_1^T + B_2 A_2^T + \dots + B_r A_r^T, \end{aligned} \quad (2)$$

where $W_i = B_i A_i^T$ is a rank-1 matrix derived from the product of the corresponding submatrices B_i and A_i .

3.2 Subspace Redundancy Formulation

Given the input $x \in \mathbb{R}^{d_{in}}$, the final output $h \in \mathbb{R}^{d_{out}}$ of the adapted module can be represented as:

$$h = h_0 + \Delta h = W_0 x + BAx. \quad (3)$$

We focus on the incremental term Δh , as it contains all trainable parameters from LoRA. Following Eq. (2), the output increment can be decomposed into a sum of rank-1 components as follows:

$$\begin{aligned} \Delta h &= BAx \\ &= B_1 A_1^T x + B_2 A_2^T x + \dots + B_r A_r^T x \\ &= \Delta h_1 + \Delta h_2 + \dots + \Delta h_r. \end{aligned} \quad (4)$$

Here, each sub-feature $\Delta h_i = B_i A_i^T x$ represents the contribution of the i -th rank-1 subspace, and A_i , B_i are the i -th column and row components from the low-rank matrices A and B , respectively.

As shown in Figure 2, the full update Δh is essentially a linear combination of the vectors B_i , modulated by the inner products between x and each A_i . This formulation allows us to interpret Δh as a composition of multiple subspace projections. To improve the expressiveness of the model, it is desirable for these subspaces to exhibit distinct characteristics. However, in practice, many of the rank-1 components are highly correlated, leading to redundancy and reduced representational diversity. We refer to this phenomenon as **feature-level redundancy** across multiple subspaces.

3.3 Subspace Regularization Formulation

To mitigate subspace redundancy, we propose a general subspace regularization term $R(B, A, X)$, where $X \in \mathbb{R}^{d_{in} \times N}$ represents a mini-batch of N input samples. ReSoRA independently applies regularization to each LoRA component, explicitly penalizing redundancy among subspaces, thereby effectively enhancing the model's adaptation capacity. Specifically, we introduce two categories of regularization methods: pairwise and set-to-set. Pairwise regularization evaluates redundancy between feature vectors, while set-to-set regularization assesses redundancy at the feature-set level, capturing structural overlaps beyond point-wise comparisons.

Table 1: Performance improvements on Flickr30K using VSE_{∞} with single Transformer (BERT + Region Features), and MSR-VTT using CLIP4Clip with dual Transformer encoders (ViT + Text Transformer). We report Recall@1 (R@1) on sentence retrieval (“I-T”, “V-T”), image retrieval (“T-I”), video retrieval (“T-V”), and “Rsum” of R@1,5,10 on bi-directional retrievals.

Method	Params. (M)	Memory (G)	BERT + Region Features			Params. (M)	Memory (G)	ViT + Text Transformer		
			I-T	T-I	Rsum			T-V	V-T	Rsum
Full	109.5	9.9	79.7	62.1	513.5	151.3	12.2 * 4	42.8	42.1	389.2
Partially	0.8	1.0	74.8	53.7	485.5	0.7	1.9 * 4	36.4	37.0	353.9
Adapter [28]	2.6	8.8	79.1	60.5	511.3	5.2	10.3 * 4	38.3	39.6	364.3
BitFit [64]	0.9	8.6	77.3	57.8	503.9	0.1	10.5 * 4	38.1	40.6	370.8
Prompt [39]	10.7	9.4	78.7	59.0	508.5	0.2	10.7 * 4	36.8	37.5	358.8
SSF [40]	0.2	8.4	80.0	60.4	512.8	0.5	9.8 * 4	40.2	41.8	376.6
FacT [31]	0.6	8.7	79.2	59.3	508.8	0.8	10.2 * 4	38.7	39.8	367.2
LST [55]	7.5	4.6	77.9	57.3	501.9	11.2	8.0 * 4	37.0	37.8	356.7
UniPT [14]	5.9	3.1	80.2	59.8	510.5	9.6	3.4 * 4	38.9	39.3	361.3
AdaLoRA [67]	1.0	8.8	79.8	60.1	510.3	1.2	10.5 * 4	39.2	39.6	368.5
LoRA [29]	1.1	8.8	78.8	59.6	508.2	1.3	10.2 * 4	38.8	39.9	366.8
+ ReSoRA	1.1	9.8	1.0 ↑	0.8 ↑	2.6 ↑	1.3	11.8 * 4	0.6 ↑	0.6 ↑	3.3 ↑

Pairwise Regularization. We first adopt commonly-used *Euclidean distance* to quantify redundancy among incremental features projected onto subspaces, denoted by Δh_i :

$$R_e(B, A, X) = \frac{1}{N} \sum_{n=1}^N \sum_{i=1}^r \sum_{j=i+1}^r e^{-\beta \|\Delta h_i^n - \Delta h_j^n\|_2^2}, \quad (5)$$

where Δh_i^n denotes the incremental output of the n -th sample projected onto the i -th subspace, and β is a scaling factor controlling feature-space sensitivity, enhancing robustness to noise.

Furthermore, we employ *Cosine distance* to capture directional differences independent of vector magnitude as follows:

$$R_c(B, A, X) = \frac{1}{N} \sum_{n=1}^N \sum_{i=1}^r \sum_{j=i+1}^r \frac{(\Delta h_i^n)^T \Delta h_j^n}{\|\Delta h_i^n\|_2 \|\Delta h_j^n\|_2}. \quad (6)$$

Set-to-set Regularization. Unlike pairwise items, set-to-set items capture global alignment and correlation across entire feature sets. We explore two well-designed regularization strategies to quantify structural similarities between different subspaces.

Specifically, *Linear measurement* (default setting) is defined as:

$$R_l(B, A, X) = \sum_{i=1}^r \sum_{j=i+1}^r \frac{\|\Delta H_i \Delta H_j^T\|_F^2}{\|\Delta H_i \Delta H_i^T\|_F \|\Delta H_j \Delta H_j^T\|_F}, \quad (7)$$

where $\Delta H_i \in \mathbb{R}^{d_{in} \times N}$ denotes batch features extracted from the i -th subspace, and $|\cdot|_F$ is the Frobenius norm.

Besides, we propose a *Nonlinear measurement* based on a kernel function to capture more complex interactions:

$$R_n(B, A, X) = \sum_{i=1}^r \sum_{j=i+1}^r \frac{\text{tr}(K_i M K_j M)}{\sqrt{\text{tr}((K_i M)^2) \text{tr}((K_j M)^2)}}, \quad (8)$$

where $M = I_N - \frac{1}{N} \mathbf{1} \mathbf{1}^T$ is a centering matrix, and $K_i(p, q) = \exp(-\|\Delta h_i^p - \Delta h_i^q\|_2^2 / (2\sigma^2))$ with variance parameter σ determined as a fraction of the median sample distances. These designs can explicitly suppress redundancy across distinct subspaces, thus substantially enhancing feature diversity and improving generalization performance in LoRA-based fine-tuning methods.

Theoretical Justification. Here we revisit the Cosine distance based regularization from Eq. (6), simplified here as:

$$R_c(B, A, X) = \sum_{i,j} \frac{(\Delta h_i)^T \Delta h_j}{\|\Delta h_i\|_2 \|\Delta h_j\|_2}. \quad (9)$$

The gradient of R_c with respect to Δh_i is derived as follows:

$$\frac{\partial R_c}{\partial \Delta h_i} = \sum_j \frac{1}{\|\Delta h_i\|_2 \|\Delta h_j\|_2} \left(\Delta h_j - \cos(\theta_{ij}) \frac{\Delta h_i}{\|\Delta h_i\|_2} \right) \quad (10)$$

where $\cos(\theta_{ij})$ denotes cosine similarity between vectors Δh_i and Δh_j . This gradient explicitly penalizes directional similarity between subspace projections. When Δh_i and Δh_j are highly aligned ($\cos(\theta_{ij}) \approx 1$), it pushes them apart, encouraging orthogonalization and reducing redundancy. This fosters feature diversity and robustness, improving generalization across tasks and domains.

4 Experiments

4.1 Experiments on Visual-Text Retrieval

Datasets. We test ReSoRA on V&L benchmarks, e.g., Flickr30K [62] on image-text retrieval, and MSR-VTT [61] on video-text retrieval.

Implementation Details. For image-text retrieval, we follow VSE_{∞} [4], employing a BERT-base encoder [10] for text and a Faster R-CNN [54] as visual extractor. For video-text retrieval, we adopt CLIP4Clip [44] as the baseline with Text Transformer [53] and ViT-B/32 [20] as the text and vision encoders. We keep their default settings, e.g., choice of optimizer, warm-up schedule, input image resolution, video sequence length, input text processing, etc.

Main Results. Table 1 shows the comparisons on image-text and video-text retrieval. Notably, ReSoRA consistently outperforms LoRA methods, achieving superior retrieval performance across different downstream tasks. It further demonstrates the general effectiveness of ReSoRA in multi-modal architectures, where its plug-and-play design better captures and aligns visual-textual relationships. Consistent gains in image-text and video-text retrieval indicate that ReSoRA serves as an effective training regularizer for low-rank adaptation, without adding inference overhead.

Table 2: Performance improvements on VTAB-1K using ViT-B/16 pre-trained on supervised ImageNet dataset.

param (M)	Natural						Specialized			Structured									sNORB-Azim	sNORB-Ele	Average	All Set Average	
	Cifar100	Caltech101	DTD	Flower102	Pets	SVHN	Sun397	Camelyon	EuroSAT	Resisc45	Retinopathy	Clevr-Count	Clevr-Dist	DMLab	KITTI-Dist	dSpr-Loc	dSpr-Ori	sNORB-Azim	sNORB-Ele				
Traditional Fine-Tuning																							
Full	85.8	68.9	87.7	64.3	97.2	86.9	87.4	38.8	79.7	95.7	84.2	73.9	56.3	58.6	41.7	65.5	57.5	46.7	25.7	29.1	68.9	65.6	
Linear	0	64.4	85.0	63.2	97.0	86.3	36.6	51.0	78.5	87.5	68.5	74.0	34.3	30.6	33.2	55.4	12.5	20.0	9.6	19.2	57.6	53.0	
PETL methods																							
BitFit [64]	0.10	72.8	87.0	59.2	97.5	85.3	59.9	51.4	78.7	91.6	72.9	69.8	61.5	55.6	32.4	55.9	66.6	40.0	15.7	25.1	65.2	62.0	
VPT [30]	0.56	78.8	90.8	65.8	98.0	88.3	78.1	49.6	81.8	96.1	83.4	68.4	68.5	60.0	46.5	72.8	73.6	47.9	32.9	37.8	72.0	69.4	
LST [55]	2.38	59.5	91.5	69.0	99.2	89.9	79.5	54.6	86.9	95.9	85.3	74.1	81.8	61.8	52.2	81.0	71.7	49.5	33.7	45.2	74.3	71.7	
AdaLoR [67]	0.44	52.1	89.1	68.9	96.8	88.2	79.5	53.6	86.5	96.1	84.4	75.6	83.0	64.1	55.9	81.6	86.4	52.7	34.4	43.5	74.6	72.2	
AdaptFormer [5]	0.16	70.8	91.2	70.5	99.1	90.9	86.6	54.8	83.0	95.8	84.4	76.3	81.9	64.3	49.3	80.3	76.3	45.7	31.7	41.1	74.7	72.3	
NOAH [69]	0.43	69.6	92.7	70.2	99.1	90.4	86.1	53.7	84.4	95.4	83.9	75.8	82.8	68.9	49.9	81.7	81.8	48.3	32.8	44.2	75.5	73.2	
SSF [40]	0.21	69.0	92.6	75.1	99.4	91.8	90.2	52.9	87.4	95.9	87.4	75.5	75.9	62.3	53.3	80.6	77.3	54.9	29.5	37.9	75.7	73.2	
FacT-TK _{r≤32} [31]	0.07	70.8	92.0	68.8	98.9	89.9	88.6	53.9	85.1	95.8	83.9	75.4	82.7	67.4	50.1	80.9	80.4	45.3	32.8	42.3	75.2	72.9	
+ ReSoRA	0.07	2.1 ↑ 0.2 ↑	1.4 ↑ 0.1 ↑	0.2 ↑ 0.3 ↑	0.4 ↑ 0.3 ↑	0.6 ↑ 0.0	0.0	0.0	0.2 ↑ 1.0 ↑	1.0 ↑ 0.7 ↑	0.7 ↑ 0.7 ↑	0.7 ↑ 0.7 ↑	0.6 ↑ 0.6 ↑	0.6 ↑ 0.6 ↑	0.6 ↑ 0.6 ↑	0.6 ↑ 0.6 ↑	0.6 ↑ 0.6 ↑	0.6 ↑ 0.6 ↑	0.6 ↑ 0.6 ↑	0.6 ↑ 0.6 ↑	0.6 ↑ 0.6 ↑	0.6 ↑ 0.6 ↑	
LoRA _{r=8} [29]	0.44	73.7	94.1	72.4	99.4	91.3	85.6	56.3	86.8	95.9	85.2	73.4	83.6	64.6	51.4	79.5	85.7	51.5	35.1	46.5	76.5	74.3	
+ ReSoRA	0.44	0.2 ↑ 0.2 ↓	0.5 ↑ 0.0	0.6 ↑ 1.9 ↑	0.4 ↑ 0.9 ↑	0.2 ↓ 1.4 ↑	1.8 ↑	0.1 ↑ 0.1 ↓	0.6 ↑ 2.6 ↑	0.8 ↑ 0.4 ↑	0.4 ↑ 0.6 ↑	0.1 ↑ 0.1 ↑	0.7 ↑ 0.7 ↑	0.7 ↑ 0.7 ↑	0.7 ↑ 0.7 ↑	0.7 ↑ 0.7 ↑	0.7 ↑ 0.7 ↑	0.7 ↑ 0.7 ↑	0.7 ↑ 0.7 ↑	0.7 ↑ 0.7 ↑	0.7 ↑ 0.7 ↑	0.7 ↑ 0.7 ↑	
MoSLoRA _{r=8} [59]	0.40	73.5	94.1	71.6	99.2	91.1	85.6	56.2	87.5	95.5	85.9	76.3	82.7	64.5	52.4	81.2	86.1	53.9	33.2	46.7	76.8	74.6	
+ ReSoRA	0.40	0.6 ↑ 0.6 ↓	0.8 ↑ 0.1 ↑	0.3 ↑ 0.9 ↑	0.4 ↑ 0.4 ↑	0.4 ↑ 0.3 ↑	0.1 ↑ 0.1 ↓	0.3 ↓ 0.3 ↓	0.9 ↑ 0.8 ↑	0.1 ↓ 0.1 ↓	0.5 ↓ 0.5 ↓	0.3 ↑ 1.1 ↑	0.5 ↓ 0.5 ↓	0.3 ↑ 0.2 ↑	0.3 ↑ 0.2 ↑	0.3 ↑ 0.2 ↑	0.3 ↑ 0.2 ↑	0.3 ↑ 0.2 ↑	0.3 ↑ 0.2 ↑	0.3 ↑ 0.2 ↑	0.3 ↑ 0.2 ↑	0.3 ↑ 0.2 ↑	
DTL+ [22]	0.04	69.9	95.0	71.5	99.3	91.8	86.8	56.8	87.8	96.1	86.4	74.7	81.6	64.9	52.0	81.7	97.0	55.0	36.4	49.6	77.5	75.5	
+ ReSoRA	0.04	0.7 ↑ 0.1 ↑	0.0	0.1 ↑ 0.0	0.9 ↑ 0.6 ↓	0.5 ↑ 0.3 ↑	0.8 ↑ 0.5 ↑	0.5 ↑ 0.1 ↓	0.4 ↑ 0.4 ↑	0.1 ↑ 0.1 ↑	0.3 ↑ 0.3 ↑	0.0	0.0	0.3 ↑ 0.1 ↑	0.4 ↑ 0.3 ↑	0.4 ↑ 0.3 ↑	0.4 ↑ 0.3 ↑	0.4 ↑ 0.3 ↑	0.4 ↑ 0.3 ↑	0.4 ↑ 0.3 ↑	0.4 ↑ 0.3 ↑	0.4 ↑ 0.3 ↑	

4.2 Experiments on VTAB-1K

Datasets. We further evaluate the effectiveness of ReSoRA on the VTAB-1K benchmark [65], a comprehensive collection of 19 diverse visual classification datasets, each containing 1,000 training samples. These datasets are categorized into three distinct groups:

(1) **Natural group:** This group includes natural image datasets from conventional cameras including CIFAR100 [37], Caltech101 [21], DTD [9], Flowers102 [50], Pets [51], Sun397 [60], and SVHN [48].

(2) **Specialized group:** This group covers imagery from specialized domains such as remote sensing and medical imaging, including Resisc45 [8], EuroSAT [27], Patch Camelyon [57], and Diabetic Retinopathy [34].

(3) **Structured group:** This group is designed to evaluate structured visual reasoning tasks, such as object counting and 3D orientation prediction. It includes CLEVR [32], dSprites [47], Small-NORB [38], DMLab [1], and KITTI [24].

Implementation Details. For VTAB-1K and few-shot experiments, we use ViT-B backbone [20] with LoRA variants under identical training settings: AdamW optimizer [43], cosine learning rate decay, batch size 32, and weight decay 5×10^{-2} . We reproduce baselines with LoRA [29], MoSLoRA [59], FacT [31], and DTL [22] for fair comparison. For LoRA and MoSLoRA, we set the rank $r = 8$, while DTL and FacT use their original configurations. ReSoRA is applied with linear set-to-set regularization by default.

Training Strategy. As PETL methods are sensitive to parameter initialization, we adopt a two-stage training strategy to ensure stable convergence and reduce variance. Following prior work [26], models are trained for 100 epochs per dataset. In stage one, baseline

PETL methods (e.g., LoRA, DTL, FacT) are trained without ReSoRA to obtain reference models; in stage two, ReSoRA with linear set-to-set regularization is introduced and trained for another 100 epochs, which is used across all experiments unless otherwise noted.

Main Results. We report top-1 accuracy for both the original models and our ReSoRA applied to various PEFT approaches, including various popular tuning methods such as LoRA [29], MoSLoRA [59], and FacT [31], as well as memory-efficient tuning methods like DTL [22], to validate ReSoRA’s effectiveness. We also compare against full fine-tuning (Full), partial tuning with a task-specific head (Linear), and competitive strategies such as BitFit [64], VPT [30], LST [55], AdaptFormer [5], NOAH [69], and SSF [40]. Finally, we include AdaLoRA [67], which reduces redundancy in LoRA by dynamically adjusting low-rank matrices during training.

The final results are summarized in Table 2, presenting a comprehensive comparison between our proposed method and existing approaches on the VTAB-1K benchmark using the ViT-B/16 backbone. The upper section of the table reports the performance of full fine-tuning and linear probing with a task-specific classification head. As shown, incorporating ReSoRA consistently enhances the baseline performance across multiple datasets without introducing additional parameters. Specifically, for LoRA, the addition of similarity regularization yields an average improvement of **0.7%** across all datasets in the grouped categories, and a similar **0.7%** gain in overall accuracy. We observe similar consistent improvements when applying ReSoRA to other PETL methods, including FacT, MoSLoRA, and DTL. These results further demonstrate its broad applicability across diverse fine-tuning strategies.

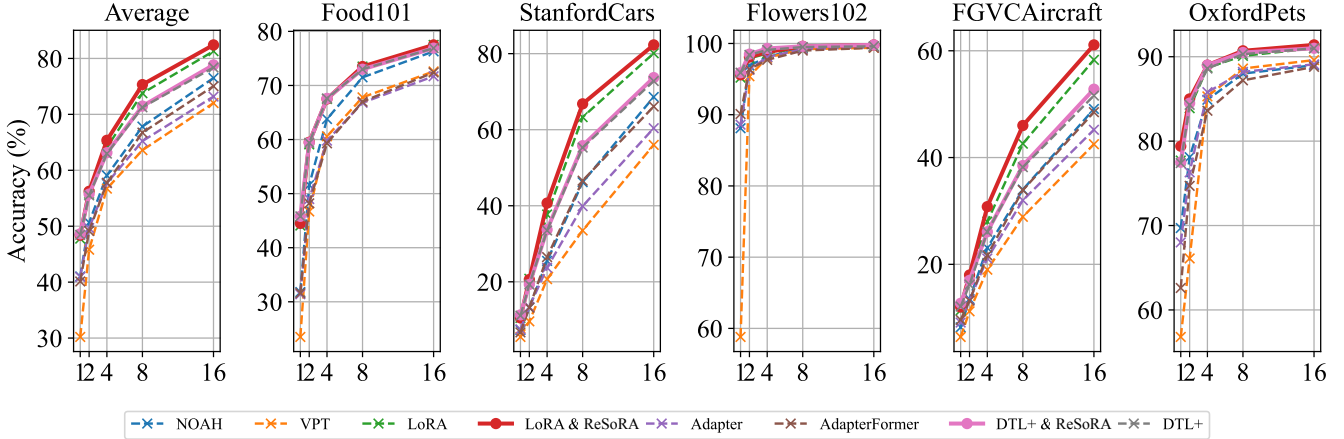


Figure 3: Few-shot results on five fine-grained recognition datasets. Solid lines indicate PELT methods with added ReSoRA; dashed lines show original results. All results are averaged over 3 seeds.

Table 3: Performance improvements on VTAB-1K using Swin Transformer and ConvNeXt pre-trained on ImageNet dataset.

Method	param(M)	Nat.	Spe.	Str.	Avg.
Swin Transformer [41]					
Full	86.7	79.2	86.2	59.7	75.0
Linear	0	73.5	80.8	33.5	62.6
BitFit [64]	0.20	74.2	80.1	42.4	65.6
VPT [30]	0.16	76.8	84.5	53.4	71.6
FacT-TK [31]	0.14	83.4	86.8	61.3	77.2
+ ReSoRA	0.14	0.2 ↓	0.4 ↑	0.5 ↑	0.2 ↑
DTL+ [22]	0.09	82.2	86.5	65.7	78.1
+ ReSoRA	0.09	0.2 ↑	0.6 ↑	0.4 ↑	0.4 ↑
ConvNeXt [42]					
LoRA [29]	0.58	82.7	85.6	64.7	77.7
+ ReSoRA	0.58	0.4 ↑	0.3 ↑	0.2 ↑	0.7 ↑

We further adopt Swin Transformer [41] and ConvNeXt [42] in Table 3 for conduct validation. Integrating ReSoRA consistently boosts the performance of these PELT methods across both Transformer and CNN architectures, demonstrating its versatility and robustness as a general enhancement for transfer learning.

4.3 Experiments on Few-shot Learning

Datasets. We conduct few-shot learning on Food101 [2], Stanford Cars [36], Flowers102 [49], FGVCAircraft [46], and OxfordPets [51]. These datasets are widely-used benchmarks for low-resource conditions and challenging fine-grained classification tasks.

Implementation Details. We follow the settings in the VTAB-1K experiments including backbone, hyperparameters, GPU hardware, and two-stage training strategy, except that we vary the number of training samples from 1-shot to 16-shot. Results are averaged over three runs with different random seeds for reliability.

Main Results. Figure 3 presents a comparison of several PELT baselines, including LoRA, DTL+, Adapter, AdaptFormer, VPT, and

Table 4: Performance improvements between feature-based and weight-based ReSoRA on VTAB-1k using ViT-B/16.

Method	param(M)	Nat.	Spe.	Str.	Avg.
Feature-Based	0.44	82.3	86.3	62.9	77.2
Weight-Based	0.44	82.2	86.1	62.5	76.9

NOAH, along with LoRA and DTL+ further enhanced by ReSoRA. The evaluation is conducted across five different datasets and shot settings (1, 2, 4, 8, 16), which test the methods under various levels of available training data. On average, ReSoRA yields a 0.5%–1% performance gain over baselines and continues to improve as training examples increase. These results demonstrate ReSoRA’s effectiveness and robustness in few-shot settings and its ability to sustain gains with more data, highlighting its value in enhancing generalization and stability for parameter-efficient transfer learning.

5 Ablation Studies

5.1 Weight vs. Feature Regularization

To compare the effectiveness of applying the same regularization at different levels, we evaluate linear set-to-set similarity regularization when applied to either the weight subspace of low-rank adaptation or the resulting feature representations.

As shown in Table 4, although applying regularization directly to the LoRA weight matrices helps mitigate redundancy within the parameter space, it consistently underperforms when compared to regularization applied at the feature level. This performance gap suggests a fundamental limitation of weight-level constraints: they influence the learned representations only implicitly and may fail to align with the underlying task semantics. In contrast, feature-level regularization provides a more direct and effective mechanism for shaping the output representations, enabling the model to better capture task-relevant variations. As a result, it leads to improved generalization and adaptability across downstream tasks.

Table 5: Performance on VTAB-1K using ViT-B/16 with LoRA under different subspace regularizations. Blue rows denote pairwise distance (Euclidean, Cosine), and green rows indicate set-to-set distance (Linear, Nonlinear). Results are reported over 19 datasets grouped into Natural, Specialized, and Structured categories. Bold values indicate the best in each rank group.

param (M)	Natural							Specialized			Structured							Average	All Set Average			
	Cifar100	Caltech101	DTD	Flower102	Pets	SVHN	Sun397	Camelyon	EuroSAT	Resisc45	Retinopathy	Clevr-Count	Clevr-Dist	DMLab	KITTI-Dist	dSpr-Loc	dSpr-Ori	sNORB-Azim	sNORB-Ele			
LoRA _{r=2} [29]	0.11	74.9	93.2	73.3	99.3	91.4	84.9	57.4	86.8	95.2	84.7	74.9	82.8	64.2	52.2	80.7	84.4	51.7	32.1	46.0	76.4	74.2
+ $R_e(B, A, X)$	0.11	75.7	93.6	73.2	99.4	91.5	87.8	57.5	87.7	95.3	85.6	74.2	83.4	64.7	53.3	80.2	84.9	52.4	32.7	46.4	76.8	74.6
+ $R_c(B, A, X)$	0.11	75.7	93.3	73.5	99.4	91.4	86.1	57.7	87.3	95.3	85.4	74.7	83.0	64.6	52.9	80.3	84.7	52.1	32.6	46.1	76.7	74.5
+ $R_n(B, A, X)$	0.11	73.4	93.4	72.7	99.4	91.4	86.3	57.7	87.0	95.2	85.7	73.2	83.1	64.6	53.3	80.7	84.9	52.1	32.3	45.5	76.6	74.5
+ $R_l(B, A, X)$	0.11	75.7	93.4	73.5	99.5	91.4	86.2	57.6	87.2	95.1	85.6	73.3	83.2	64.7	52.8	81.3	85.1	52.6	32.9	46.5	76.7	74.6
LoRA _{r=4} [29]	0.22	74.5	93.9	71.4	99.3	91.4	83.6	56.8	87.2	95.5	85.7	75.3	83.2	65.0	52.3	81.3	85.8	52.4	33.0	46.0	76.6	74.4
+ $R_e(B, A, X)$	0.22	74.9	93.7	72.3	99.4	91.5	85.3	56.9	88.0	95.9	86.4	75.4	83.3	65.5	52.9	81.6	86.8	53.0	34.0	45.6	77.1	74.9
+ $R_c(B, A, X)$	0.22	74.9	93.7	72.4	99.4	91.1	85.0	57.0	87.6	95.9	86.1	75.3	82.8	65.6	52.9	82.0	86.5	52.8	33.8	45.4	77.0	74.7
+ $R_n(B, A, X)$	0.22	75.2	93.6	72.1	99.4	91.6	85.3	57.6	87.4	95.9	86.7	75.3	83.0	65.6	53.3	81.4	86.7	52.6	33.4	45.7	77.1	74.8
+ $R_l(B, A, X)$	0.22	75.4	93.6	72.1	99.4	91.6	85.1	57.2	87.7	96.0	86.4	75.3	83.1	65.5	53.2	81.7	86.8	53.0	33.8	45.2	77.1	74.9
LoRA _{r=8} [29]	0.44	73.7	94.1	72.4	99.4	91.3	85.6	56.3	86.8	95.9	85.2	73.4	83.6	64.6	51.4	79.5	85.7	51.5	35.1	46.5	76.5	74.3
+ $R_e(B, A, X)$	0.44	73.6	93.1	72.2	99.2	91.0	87.4	56.5	87.7	95.6	86.1	74.7	82.7	64.3	51.6	81.6	86.0	52.0	35.7	44.8	76.7	74.5
+ $R_c(B, A, X)$	0.44	73.9	93.3	72.7	99.3	91.4	87.0	56.7	87.5	95.7	86.3	73.5	82.7	64.7	51.4	80.6	85.7	51.7	35.6	46.1	76.7	74.5
+ $R_n(B, A, X)$	0.44	74.0	93.9	72.7	99.3	91.7	86.7	56.7	87.8	95.8	86.5	74.2	82.9	64.5	51.4	80.9	85.8	52.7	35.3	46.1	76.8	74.6
+ $R_l(B, A, X)$	0.44	73.9	93.9	72.9	99.4	91.9	87.5	56.7	87.7	95.7	86.6	75.2	83.7	64.5	52.0	82.1	86.5	51.9	35.7	46.6	77.2	75.0

5.2 Comparisons of Different Regularization

To better understand the role of different regularizations, we conduct a comprehensive study on the ViT-B/16 backbone with LoRA of varying ranks ($n = 2, 4, 8$). We compare pairwise distance measures (e.g., Euclidean and cosine distance) with set-to-set approaches based on Linear and Nonlinear distance formulations.

As shown in Table 5, applying pairwise regularization techniques, such as Euclidean distance and cosine distance, to the incremental features proves to be effective in reducing redundancy across various LoRA ranks. Notably, even in the low-rank setting ($r = 2$), where the rank is minimal, significant redundancy persists. This finding suggests that the overlap of subspaces is not solely a consequence of high-rank configurations. Instead, it highlights that subspace redundancy is an inherent issue that can occur across all rank configurations, not just in higher-dimensional settings. This indicates that the redundancy problem is fundamental and needs to be addressed regardless of the rank dimension.

At higher ranks (e.g., $n = 4, n = 8$), the performance gains of pairwise regularization become more pronounced, particularly on datasets such as SVHN and KITTI. Besides, the set-to-set regularization, including both linear and nonlinear items, further improves performance by encouraging more compact and discriminative feature subspaces. Compared to pairwise methods, set-to-set regularization shows greater robustness to input variations and consistently yields stronger results in more complex scenarios.

Overall, both regularization forms play a crucial role in reducing redundancy within LoRA parameters and boosting adaptation performance. Among all the strategies evaluated, the linear set-to-set item stands out by delivering the most significant improvements, indicating its superior ability to enforce diversity and enhance the representational capacity of the learned subspaces.

Table 6: Memory and resource analyses of different ReSoRA variants on VTAB-1K using ViT-B/16 backbone.

Method	Mem (GB)	FLOPs (T)	Time (%)	Acc (%)
Full	4.9	0.54	-	68.9
LoRA [29]	3.4	0.56	100	76.4
+ $R_e(B, A, X)$	3.4	0.83	+18	0.4 ↑
+ $R_c(B, A, X)$	4.0	0.83	+32	0.3 ↑
+ $R_n(B, A, X)$	4.0	0.83	+34	0.2 ↑
+ $R_l(B, A, X)$	4.0	0.83	+34	0.3 ↑
DTL [22]	2.4	0.56	100	77.5
+ $R_e(B, A, X)$	2.5	0.65	+14	0.2 ↑
+ $R_c(B, A, X)$	3.0	0.65	+32	0.3 ↑
+ $R_n(B, A, X)$	3.0	0.65	+32	0.4 ↑
+ $R_l(B, A, X)$	3.0	0.65	+32	0.4 ↑

5.3 Memory and Resource Usage

To thoroughly assess ReSoRA’s efficiency, we compare memory usage, computational cost (FLOPs/iteration), training time, and accuracy across different forms, evaluating pairwise (Euclidean: R_e , Cosine: R_c) and set-to-set (Linear: R_l , Nonlinear: R_n) variants.

Table 6 summarizes the results. Compared to baseline LoRA [29] and DTL [22], our ReSoRA consistently improves accuracy by approximately 0.2% to 0.4% across different configurations. In particular, these performance improvements are achieved with minimal additional memory usage (at most 0.6 GB) and a modest increase in training time (ranging from 14% to 34%), while introducing no extra inference overhead. Although the linear set-to-set form (R_l) generally achieves better performance, the Euclidean pairwise form (R_e) offers a balance between accuracy and computational efficiency.

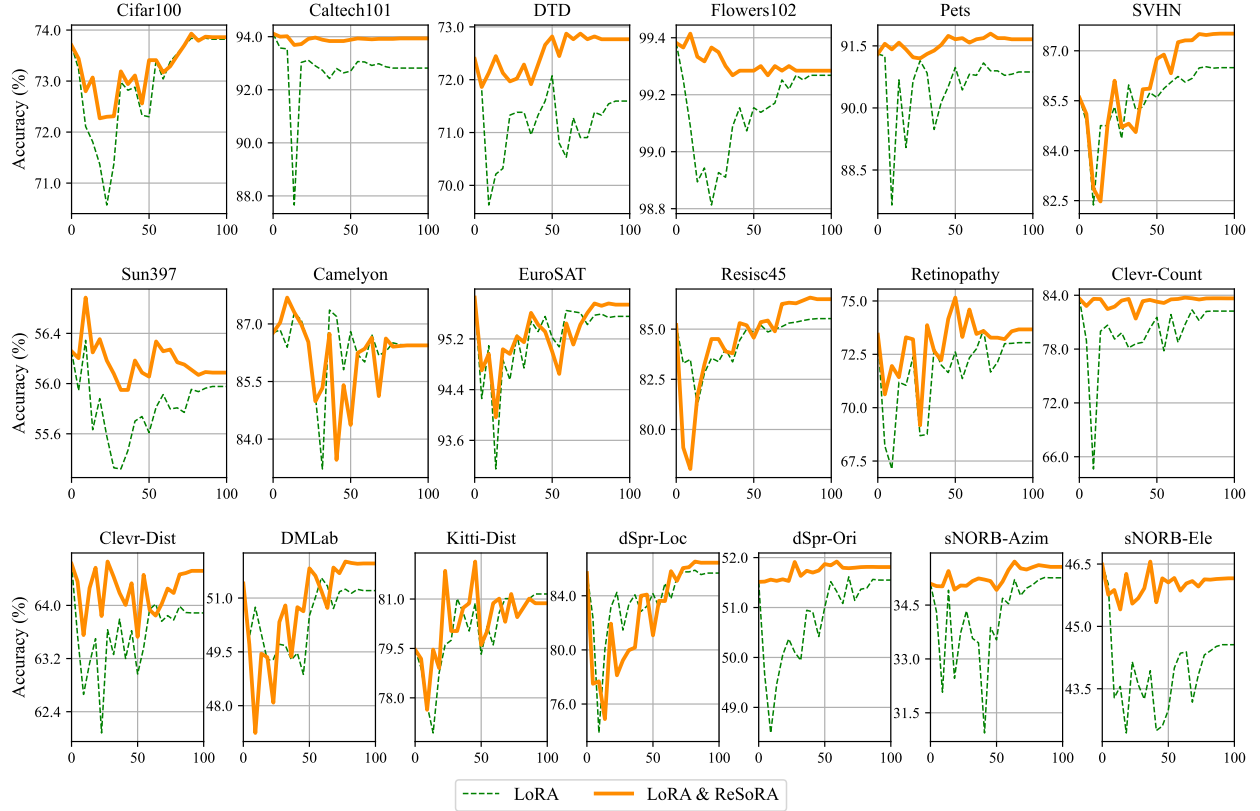


Figure 4: Effective training by adding ReSoRA in the second stage. The curves show test accuracy across datasets during training.

5.4 Effective Training of ReSoRA

To validate the training configurations for the proposed ReSoRA, we perform ablation studies using the ViT-B/16 backbone with trainable LoRA adapters on the VTAB-1k benchmark. As illustrated in Figure 4, we compare the top-1 accuracy during the second stage of training between models optimized with the original objective and those enhanced by our regularization strategy.

In Figure 4, models trained solely with the original loss function experience a noticeable drop in accuracy during the second training stage, which reflects an overfitting issue caused by insufficient regularization. In contrast, our ReSoRA not only mitigates this degradation but also pushes performance beyond the baseline levels. On datasets such as Caltech101 [21], Pets [51], Clevr-Count [32], dSpr-Ori [47], and sNORB-Azim [38], the regularized models exhibit faster convergence and achieve higher accuracy early in training, demonstrating the strong stabilizing effect of ReSoRA.

For more challenging datasets, including Resisc45 [8], DMLab [1], and dSpr-Loc [47], we discover that performance gains continue to improve steadily as the subspace is progressively refined, ultimately surpassing the baseline results. These observations underscore the effectiveness of ReSoRA as a post-stage training strategy, which is adopted as the default configuration across all our experiments to ensure consistent gains and robust generalization.

6 Conclusion

In this paper, we propose **ReSoRA**, a simple yet highly effective method for reducing parameter redundancy in low-rank adaptation. Specifically, ReSoRA works by decomposing the output space of the adaptive branch into multiple subspaces, allowing for more targeted and efficient adaptation. To encourage diversity among these subspaces, ReSoRA introduces a regularization term that penalizes similarity across them, fostering better feature representation and enhancing the model's adaptability. Extensive experiments on vision-text retrieval and visual classification tasks demonstrate that our ReSoRA consistently improves various baseline models and application scenarios, particularly in low-data and few-shot settings. Moreover, it integrates seamlessly with existing LoRA-like methods without adding inference overhead. These results validate its effectiveness and establish it as a promising, general solution for efficient fine-tuning across diverse domains and tasks.

Discussion. We present ReSoRA as a novel, effective, and easy-to-implement regularization technique for low-rank adaptation across diverse backbones and application domains. A current limitation is its role as a post-training refinement step, which adds extra training time. In the future, we plan to integrate ReSoRA into larger-scale foundation models and generative AI pipelines as better computational resources and high-quality data become available.

Acknowledgements. This paper is supported in part by the National Natural Science Foundation of China under Grant Nos. 62441231 and 62293542, the Liaoning Province Science and Technology Plan under Grant No. 2023JH26/10200016, the Dalian City Science and Technology Innovation Fund under Grant No. 2023JJ11CG001, the Natural Science Foundation of Zhejiang Province under Grant No. LD25F020001, and the Ningbo Key R&D Project under Grant No. 2025Z039, and in part by the Grant 2024-0011(ZX20240867).

References

- [1] Charles Beattie, Joel Z Leibo, Denis Teplyashin, Tom Ward, Marcus Wainwright, Heinrich Küttler, Andrew Lefrancq, Simon Green, Victor Valdés, Amir Sadik, et al. 2016. Deepmind lab. *arXiv:1612.03801* (2016).
- [2] Lukas Bossard, Matthieu Guillaumin, and Luc Van Gool. 2014. Food-101-mining discriminative components with random forests. In *ECCV*. Springer, 446–461.
- [3] Tom Brown, Benjamin Mann, Nick Ryder, Melanie Subbiah, Jared D Kaplan, Prafulla Dhariwal, Arvind Neelakantan, Pranav Shyam, Girish Sastry, Amanda Askell, et al. 2020. Language models are few-shot learners. *Advances in neural information processing systems* 33 (2020), 1877–1901.
- [4] Jiacheng Chen, Hexiang Hu, Hao Wu, Yuning Jiang, and Changhu Wang. 2021. Learning the Best Pooling Strategy for Visual Semantic Embedding. In *CVPR*. 15789–15798.
- [5] Shoufa Chen, Chongjian Ge, Zhan Tong, Jiangliu Wang, Yibing Song, Jue Wang, and Ping Luo. 2022. Adapformer: Adapting vision transformers for scalable visual recognition. *Advances in Neural Information Processing Systems* 35 (2022), 16664–16678.
- [6] Xiangyu Chen, Jing Liu, Ye Wang, Matthew Brand, Guanghui Wang, Toshiaki Koike-Akino, et al. 2024. SuperLoRA: Parameter-Efficient Unified Adaptation of Multi-Layer Attention Modules. *arXiv:2403.11887* (2024).
- [7] Zhe Chen, Yuchen Duan, Wenhui Wang, Junjun He, Tong Lu, Jifeng Dai, and Yu Qiao. 2023. Vision Transformer Adapter for Dense Predictions. In *ICLR*.
- [8] Gong Cheng, Junwei Han, and Xiaoqiang Lu. 2017. Remote sensing image scene classification: Benchmark and state of the art. *Proc. IEEE* 105, 10 (2017), 1865–1883.
- [9] Mircea Cimpoi, Subhransu Maji, Iasonas Kokkinos, Sammy Mohamed, and Andrea Vedaldi. 2014. Describing textures in the wild. In *CVPR*. 3606–3613.
- [10] Jacob Devlin, Ming-Wei Chang, Kenton Lee, and Kristina Toutanova. 2019. BERT: Pre-training of Deep Bidirectional Transformers for Language Understanding. In *NAACL*. 4171–4186.
- [11] Haiwen Diao, Yufeng Cui, Xiaotong Li, Yueze Wang, Huchuan Lu, and Xinlong Wang. 2024. Unveiling Encoder-Free Vision-Language Models. In *NeurIPS*.
- [12] Haiwen Diao, Xiaotong Li, Yufeng Cui, Yueze Wang, Haoge Deng, Ting Pan, Wenzuan Wang, Huchuan Lu, and Xinlong Wang. 2025. EVEv2: Improved Baselines for Encoder-Free Vision-Language Models. *arXiv:2502.06788* (2025).
- [13] Haiwen Diao, Bo Wan, Xu Jia, Yunzhi Zhuge, Ying Zhang, Huchuan Lu, and Long Chen. 2025. SHERL: Synthesizing High Accuracy and Efficient Memory for Resource-Limited Transfer Learning. In *ECCV*. 75–95.
- [14] Haiwen Diao, Bo Wan, Ying Zhang, Xu Jia, Huchuan Lu, and Long Chen. 2024. UniPT: Universal Parallel Tuning for Transfer Learning with Efficient Parameter and Memory. In *CVPR*.
- [15] Haiwen Diao, Ying Zhang, Shang Gao, Jiawen Zhu, Long Chen, and Huchuan Lu. 2024. GSSF: Generalized Structural Sparse Function for Deep Cross-Modal Metric Learning. *TIP* 33 (2024), 6241–6252.
- [16] Ning Ding, Xingtai Lv, Qiaosen Wang, Yulin Chen, Bowen Zhou, Zhiyuan Liu, and Maosong Sun. 2023. Sparse Low-rank Adaptation of Pre-trained Language Models. In *EMNLP*.
- [17] Wei Dong, Yuan Sun, Yiting Yang, Xing Zhang, Zhijun Lin, Qingsen Yan, Haokui Zhang, Peng Wang, Yang Yang, and Hengtao Shen. 2024. Efficient Adaptation of Pre-trained Vision Transformer via Householder Transformation. *arXiv:2410.22952* (2024).
- [18] Wei Dong, Dawei Yan, Zhijun Lin, and Peng Wang. 2023. Efficient adaptation of large vision transformer via adapter re-composing. *Advances in Neural Information Processing Systems* 36 (2023), 52548–52567.
- [19] Wei Dong, Xing Zhang, Bihui Chen, Dawei Yan, Zhijun Lin, Qingsen Yan, Peng Wang, and Yang Yang. 2024. Low-rank rescaled vision transformer fine-tuning: A residual design approach. In *Proceedings of the IEEE/CVF Conference on Computer Vision and Pattern Recognition*. 16101–16110.
- [20] Alexey Dosovitskiy, Lucas Beyer, Alexander Kolesnikov, Dirk Weissenborn, Xiaohua Zhai, Thomas Unterthiner, Mostafa Dehghani, Matthias Minderer, Georg Heigold, Sylvain Gelly, Jakob Uszkoreit, and Neil Houlsby. 2021. An Image is Worth 16x16 Words: Transformers for Image Recognition at Scale. In *ICLR*.
- [21] Li Fei-Fei, Robert Fergus, and Pietro Perona. 2006. One-shot learning of object categories. *PAMI* 28, 4 (2006), 594–611.
- [22] Minghao Fu, Ke Zhu, and Jianxin Wu. 2024. Dtl: Disentangled transfer learning for visual recognition. In *AAAI*, Vol. 38. 12082–12090.
- [23] Peng Gao, Shijie Geng, Renrui Zhang, Teli Ma, Rongyao Fang, Yongfeng Zhang, Hongsheng Li, and Yu Qiao. 2021. CLIP-Adapter: Better Vision-Language Models with Feature Adapters. *arXiv: 2110.04544* (2021).
- [24] A Geiger, P Lenz, C Stiller, and R Urtasun. 2013. Vision meets robotics: The KITTI dataset. *The International Journal of Robotics Research* (2013), 1–6.
- [25] Demi Guo, Alexander M. Rush, and Yoon Kim. 2021. Parameter-Efficient Transfer Learning with Diff Pruning. In *ACL*. 4884–4896.
- [26] Haoyu He, Jianfei Cai, Jing Zhang, Dacheng Tao, and Bohan Zhuang. 2023. Sensitivity-aware visual parameter-efficient fine-tuning. In *ICCV*. 11825–11835.
- [27] Patrick Helber, Benjamin Bischke, Andreas Dengel, and Damian Borth. 2019. Eurosat: A novel dataset and deep learning benchmark for land use and land cover classification. *IEEE Journal of Selected Topics in Applied Earth Observations and Remote Sensing* 12, 7 (2019), 2217–2226.
- [28] Neil Houlsby, Andrei Giurgiu, Stanislaw Jastrzebski, Bruna Morrone, Quentin de Laroussilhe, Andrea Gesmundo, Mona Attaryan, and Sylvain Gelly. 2019. Parameter-Efficient Transfer Learning for NLP. In *ICML (Proceedings of Machine Learning Research)*, Vol. 97. 2790–2799.
- [29] Edward J. Hu, Yelong Shen, Phillip Wallis, Zeyuan Allen-Zhu, Yuanzhi Li, Shean Wang, Lu Wang, and Weizhi Chen. 2022. LoRA: Low-Rank Adaptation of Large Language Models. In *ICLR*.
- [30] Menglin Jia, Luming Tang, Bor-Chun Chen, Claire Cardie, Serge J. Belongie, Bharath Hariharan, and Ser-Nam Lim. 2022. Visual Prompt Tuning. In *ECCV*, Vol. 13693. 709–727.
- [31] Shibo Jie and Zhi-Hong Deng. 2023. FacT: Factor-Tuning for Lightweight Adaptation on Vision Transformer. In *AAAI*.
- [32] Justin Johnson, Bharath Hariharan, Laurens Van Der Maaten, Li Fei-Fei, C Lawrence Zitnick, and Ross Girshick. 2017. Clevr: A diagnostic dataset for compositional language and elementary visual reasoning. In *CVPR*. 2901–2910.
- [33] Chen Ju, Tengda Han, Kunhao Zheng, Ya Zhang, and Weidi Xie. 2022. Prompting Visual-Language Models for Efficient Video Understanding. In *ECCV*, Vol. 13695. 105–124.
- [34] EyePacs Kaggle. 2015. Kaggle Diabetic Retinopathy Detection. <https://www.kaggle.com/c/diabetic-retinopathy-detection> Accessed: Sep. 12, 2024.
- [35] Konwoo Kim, Michael Laskin, Igor Mordatch, and Deepak Pathak. 2021. How to Adapt Your Large-Scale Vision-and-Language Model. *openreview* (2021).
- [36] Jonathan Krause, Michael Stark, Jia Deng, and Li Fei-Fei. 2013. 3d object representations for fine-grained categorization. In *ICCVW*. 554–561.
- [37] Alex Krizhevsky, Geoffrey Hinton, et al. 2009. Learning multiple layers of features from tiny images. (2009).
- [38] Yann LeCun, Fu Jie Huang, and Leon Bottou. 2004. Learning methods for generic object recognition with invariance to pose and lighting. In *CVPR*, Vol. 2. IEEE, II–104.
- [39] Xiang Lisa Li and Percy Liang. 2021. Prefix-Tuning: Optimizing Continuous Prompts for Generation. In *ACL*. 4582–4597.
- [40] Dongze Lian, Daquan Zhou, Jia Shi Feng, and Xinchao Wang. 2022. Scaling & Shifting Your Features: A New Baseline for Efficient Model Tuning. In *NeurIPS*.
- [41] Ze Liu, Yutong Lin, Yue Cao, Han Hu, Yixuan Wei, Zheng Zhang, Stephen Lin, and Baining Guo. 2021. Swin Transformer: Hierarchical Vision Transformer using Shifted Windows. In *ICCV*. IEEE, 9992–10002.
- [42] Zhuang Liu, Hanzi Mao, Chao-Yuan Wu, Christoph Feichtenhofer, Trevor Darrell, and Saining Xie. 2022. A convnet for the 2020s. In *CVPR*. 11976–11986.
- [43] Ilya Loshchilov, Frank Hutter, et al. 2017. Fixing weight decay regularization in adam. *arXiv:1711.05101* 5 (2017).
- [44] Huaiashuo Luo, Lei Ji, Ming Zhong, Yang Chen, Wen Lei, Nan Duan, and Tianrui Li. 2021. CLIP4Clip: An Empirical Study of CLIP for End to End Video Clip Retrieval. *arXiv: 2104.08860* (2021).
- [45] Rabeeh Karimi Mahabadi, James Henderson, and Sebastian Ruder. 2021. Compcat: Efficient Low-Rank Hypercomplex Adapter Layers. In *NeurIPS*. 1022–1035.
- [46] Subhransu Maji, Esa Rahtu, Juho Kannala, Matthew Blaschko, and Andrea Vedaldi. 2013. Fine-grained visual classification of aircraft. *arXiv:1306.5151* (2013).
- [47] Loic Matthey, Irina Higgins, Demis Hassabis, and Alexander Lerchner. 2017. dsprites: Disentanglement testing sprites dataset.
- [48] Yuval Netzer, Tao Wang, Adam Coates, Alessandro Bissacco, Baolin Wu, Andrew Y Ng, et al. 2011. Reading digits in natural images with unsupervised feature learning. In *NIPS workshop on deep learning and unsupervised feature learning*, Vol. 2011. Granada, 4.
- [49] M.-E. Nilsback and A. Zisserman. 2006. A Visual Vocabulary for Flower Classification. In *CVPR*, Vol. 2. 1447–1454. doi:10.1109/CVPR.2006.42
- [50] Maria-Elena Nilsback and Andrew Zisserman. 2008. Automated flower classification over a large number of classes. In *2008 Sixth Indian conference on computer vision, graphics & image processing*. IEEE, 722–729.
- [51] Omkar M Parkhi, Andrea Vedaldi, Andrew Zisserman, and CV Jawahar. 2012. Cats and dogs. In *CVPR*. IEEE, 3498–3505.
- [52] Alec Radford, Jong Wook Kim, Chris Hallacy, Aditya Ramesh, Gabriel Goh, Sandhini Agarwal, Girish Sastry, Amanda Askell, Pamela Mishkin, Jack Clark, Gretchen Krueger, and Ilya Sutskever. 2021. Learning Transferable Visual Models From Natural Language Supervision. In *ICML*, Vol. 139. 8748–8763.

[53] Alec Radford, Jeffrey Wu, Rewon Child, David Luan, Dario Amodei, Ilya Sutskever, et al. 2019. Language models are unsupervised multitask learners. *OpenAI blog* 1, 8 (2019), 9.

[54] Shaogang Ren, Kaiming He, Ross B. Girshick, and Jian Sun. 2015. Faster R-CNN: Towards Real-Time Object Detection with Region Proposal Networks. In *NIPS*. 91–99.

[55] Yi-Lin Sung, Jaemin Cho, and Mohit Bansal. 2022. LST: Ladder Side-Tuning for Parameter and Memory Efficient Transfer Learning. In *NeurIPS*.

[56] Yi-Lin Sung, Jaemin Cho, and Mohit Bansal. 2022. VL-ADAPTER: Parameter-Efficient Transfer Learning for Vision-and-Language Tasks. In *CVPR*. 5217–5227.

[57] Bastiaan S Veeling, Jasper Linmans, Jim Winkens, Taco Cohen, and Max Welling. 2018. Rotation equivariant CNNs for digital pathology. In *MICCAI*. Springer, 210–218.

[58] Junjie Wang, Guangjing Yang, Wentao Chen, Huahui Yi, Xiaohu Wu, and Qicheng Lao. 2024. MLAE: Masked LoRA Experts for Parameter-Efficient Fine-Tuning. *arXiv:2405.18897* (2024).

[59] Taiqiang Wu, Jiahao Wang, Zhe Zhao, and Ngai Wong. 2024. Mixture-of-Subspaces in Low-Rank Adaptation. *arXiv:2406.11909* (2024).

[60] Jianxiong Xiao, James Hays, Krista A Ehinger, Aude Oliva, and Antonio Torralba. 2010. Sun database: Large-scale scene recognition from abbey to zoo. In *CVPR*. IEEE, 3485–3492.

[61] Jun Xu, Tao Mei, Ting Yao, and Yong Rui. 2016. MSR-VTT: A Large Video Description Dataset for Bridging Video and Language. In *CVPR*. 5288–5296.

[62] Peter Young, Alice Lai, Micah Hodosh, and Julia Hockenmaier. 2014. From image descriptions to visual denotations: New similarity metrics for semantic inference over event descriptions. *TACL* 2 (2014), 67–78.

[63] Jiazu Yu, Haomiao Xiong, Lu Zhang, Haiwen Diao, Yunzhi Zhuge, Lanqing Hong, Dong Wang, Huchuan Lu, You He, and Long Chen. 2024. LLMs Can Evolve Continually on Modality for X-Modal Reasoning. In *NeurIPS*.

[64] Elad Ben Zaken, Yoav Goldberg, and Shauli Ravfogel. 2022. BitFit: Simple Parameter-efficient Fine-tuning for Transformer-based Masked Language-models. In *ACL*. 1–9.

[65] Xiaohua Zhai, Joan Puigcerver, Alexander Kolesnikov, Pierre Ruyssen, Carlos Riquelme, Mario Lucic, Josip Djolonga, Andre Susano Pinto, Maxim Neumann, Alexey Dosovitskiy, et al. 2019. A large-scale study of representation learning with the visual task adaptation benchmark. *arXiv:1910.04867* (2019).

[66] Feiyu Zhang, Liangzhi Li, Junhao Chen, Zhouqiang Jiang, Bowen Wang, and Yiming Qian. 2023. Incretora: Incremental parameter allocation method for parameter-efficient fine-tuning. *arXiv:2308.12043* (2023).

[67] Qingru Zhang, Minshuo Chen, Alexander Bukharin, Pengcheng He, Yu Cheng, Weizhu Chen, and Tuo Zhao. 2023. Adaptive Budget Allocation for Parameter-Efficient Fine-Tuning. In *ICLR*.

[68] Ruiyi Zhang, Rushi Qiang, Sai Ashish Somayajula, and Pengtao Xie. 2024. AutoLoRA: Automatically Tuning Matrix Ranks in Low-Rank Adaptation Based on Meta Learning. *arXiv:2403.09113* (2024).

[69] Yuanhan Zhang, Kaiyang Zhou, and Ziwei Liu. 2022. Neural Prompt Search. *arXiv: 2206.04673* (2022).

[70] Yue Zhu, Haiwen Diao, Shang Gao, Long Chen, and Huchuan Lu. 2025. KARST: Multi-Kernel Kronecker Adaptation with Re-Scaling Transmission for Visual Classification. In *ICASSP*. 1–5.

[71] Yun Zhu, Nevan Wickers, Chu-Cheng Lin, Xinyi Wang, Tianlong Chen, Lei Shu, Han Lu, Canoe Liu, Liangchen Luo, Jindong Chen, et al. 2023. Sira: Sparse mixture of low rank adaptation. *arXiv:2311.09179* (2023).